IEEE Access
Multidisciplinary | Rapid Review | Open Access Journal

Received August 16, 2019, accepted August 27, 2019, date of publication September 9, 2019,
date of current version September 25, 2019.

Digital Object Identifier 10.1109/ACCESS.2019.2940054

Signal Fuse Learning Method With Dual Bands WiFi Signal Measurements in Indoor Positioning

CHUNG-MING OWN, (Member, IEEE), JIAWANG HOU, AND WENYUAN TAO
College of Intelligence and Computing, Tianjin University, Tianjin 300350, China
Corresponding author: Wenyuan Tao (taowenyuan@tju.edu.cn)

ABSTRACT Today, indoor localization technology based on WiFi signals has become more and more popular and applicable. It not only facilitates people's lives but also creates enormous economic value. However, during the propagation of the WiFi signal, it is easily interfered by obstacles, and the signal fluctuation is significant, resulting in low accuracy of positioning. To overcome these problems, we reduce the influence of environmental factors firstly. Then the positioning accuracy is improved by using the SVM model to distinguish the NLOS or LOS environment and employing the capsule networks to derive the users' positions with the WiFi 2.4G and 5G signals. As we all know, the WiFi 2.4G signal has excellent penetrability and is less affected by obstacles, while the WiFi 5G signal has excellent stability and small fluctuations. Therefore, we use the advantages of these two kinds of signals to derive the optimal suggestion by the capsule neural network, which is the learning system with minimum data sets needed. The experimental results show that the positioning effect of the two signals simultaneously is better than the positioning effect of a single signal. We also compare with the traditional indoor positioning methods and use the simulation data to carry out the robustness test, and the positioning accuracy reached 0.99 m in the field environment finally.

INDEX TERMS Indoor localization, NLOS and LOS channel propagation condition, WiFi 2.4G and WiFi 5G, SVM, capsule network.

I. INTRODUCTION

Since the 21st century, various science and technology have flourished. Research in the fields of artificial intelligence, big data, and the Internet of Things has been widely used in human life and production, creating enormous wealth. In recent years, many positioning technologies developed as the IoT system have been proposed, such as Radio Frequency [1], [2], Infrared [3], Ultrasound [4]–[8], Optical, and Magnetic Field Strength [9]–[12] with the relevant positioning calculation mechanism. This kind of positioning mainly includes two application scenarios. The first scenario is a kind of outdoor positioning. The technology of outdoor positioning has been significantly improved over the past few decades. The more representative technologies are cellular positioning and GPS technology [13]. These technologies have become extremely mature and reliable after long periods of use and countless people. Through these technologies, we are able to enjoy many conveniences. But unfortunately, GPS and other technologies cannot be applied to indoor environments, and the positioning effect is very poor. The reason is the complexity of the environment and the difficulty at the penetrating of the GPS signal. Especially, the signal decays and absorbs by the moving/stable obstacles.

In indoor positioning systems, in addition to high precision requirements, low cost, low complexity, and short time consumption are also important indicators. Nowadays, internet technology is developing rapidly, WiFi networks are becoming more and more popular, and its coverage is becoming wider and wider. Therefore, WiFi-based indoor positioning technology has become more and more popular due to its simplicity, low cost (no additional hardware required), and many commercial applications for indoor positioning are based on WiFi [14]–[20]. Generally, most of the research on WiFi fingerprint location technology is based on the signal of WiFi 2.4GHz frequency (2.4G for short). For example, Xuke Hu proposed the concept of AP (access point) set similarity, and used the WKNN algorithm to classify k nearest neighbors [21]. In recent years, the technology on WiFi 5GHz frequency (5G for short) has been appeared. Considering the stability of the WiFi 5G signal, which is not easily disturbed by environment factors, Feng Yu uses the WiFi 5G signals

The associate editor coordinating the review of this manuscript and approving it for publication was Min Jia.

and cluster KNN algorithm to achieve indoor positioning. Yu found that the positioning accuracy and efficiency using WiFi 5G are significantly improved than 2.4G [22]. Meanwhile, Arsham Farshad also proved that the WiFi 5G signal is more stable than the 2.4G, and the positioning result is also more accurate than using 2.4G with the new ideas of virtual access points [23]. Besides, Kyeong Soo Kim et al. proposed a new DNN architecture for the reduction of feature space dimension, which the multi-building and multi-floor indoor localization system based on WiFi fingerprinting is built based on the feed-forward classifier for multi-label classification [24].

Recently, Cai et al. applied the convolutional neural network as the solution to indoor positioning. In their research, the original channel state information (CSI) is used as the input into the convolutional neural network (CNN) without manually extracting the data features, which achieves a good positioning effect. However, the data of network input is derived in a very high dimension, and the implemented based on WiFi is required more APs, thus, the computation cost is very high [25]. Furthermore, with the growing of architectural space, the cause of the location complexity would decrease the positioning accuracy, and the adding labels for the CNN is another trouble at the making model [24]. To solve the above problem, Fei Teng et al. used a deep Gaussian regression model for indoor positioning. This model is a nonparametric model, and it only needs to measure part of the reference points, thus reducing the time and cost required for data collection [26]. However, according to our investigation, their researches all are based on the 2.4G signal band. The advantage of the WiFi channel band is not revealed.

In this paper, we proposed the fuse learning method with the dual bands on the WiFi positioning system, our system named as BiCN method (Bi-modal capsule network for indoor localization using commodity WiFi devices). In BiCN, we collect WiFi 2.4G and 5G signals from the APs that are preset and used to build the fingerprint database on these dual bands firstly. In our training phase, we extract the four characterizing values of the WiFi signal, including the mean, the variance, the kurtosis, and the skewness from the original data, and manually tag the feature values of each signal to identify the received signal in NLOS condition or LOS condition [27]–[31]. Accordingly, our learning model is the capsule network model. The capsule neural network was proposed by Hinton, the proponent of the convolutional neural network, in 2017 [32]. In terms of image processing, the amount of training data required is much smaller than that of CNN, but the effect is not inferior to CNN, which is the advantage of the capsule network. In this paper, the capsule network is employed by the ability to handling low-dimensional data, and the amount of data required for training is small, which is better than other DNN networks. Thus, when training the capsule network model, the input of WiFi 2.4G and 5G signal data are used in the dual capsule networks for training, because the first layer in the capsule network is the convolution layer, that is why we called the proposed model as bi-model.

The contributions of this study include three aspects as follows:

First, we theoretically and experimentally validate the feasibility of using bi-modal WiFi data for indoor localization. To our best knowledge, our proposed study is the first method to use WiFi 2.4GHz and 5GHz together with the distinct NLOS and LOS conditions.

Second, we propose the capsule network for the indoor fingerprinting firstly. The traditional neural networks need a large training dataset, but the capsule network can achieve a good effect by training with small and low-dimensional data. According to our experience, the inference process really fits the small quantity of APs and reduces the computation cost.

Third, because of the complementation properties of 2.4G and 5G, our proposed strength the signal on different frequency on the dual bands WiFi APs to predict the user location in different typical scenarios. Our experiments' results show that the proposed BiCN can outperform at some representative existing schemes with the high localization accuracy.

The remainder of this paper is organized as follows. Section 2 introduces the characteristics of dual bands WiFi. Section 3 specifies the system architecture and theoretical basis. The experimental process, performance comparison, and localization error analyses are described in Section 4. Finally, the conclusion is drawn in Section 5.

II. PRELIMINARIES

A. CONDITIONS OF LOS AND NLOS

The concept of location fingerprinting is that the location in the environment is associated with certain fingerprint, and one location corresponds to a unique fingerprint. In our study, the fingerprint is the received signal strength (RSS) value at the fixed location. Generally, the RSS value received by the mobile phone is unique at every location, like a human fingerprint. It is usually necessary to establish a fingerprint database for position matching or training models in the fingerprint localization method. Besides, the disadvantage of the fingerprint is that the RSS values are affected by the environment factors, such as obstacles blocking, temperature and humidity. The positioning effect is suffered by the state of signal blocking, called NLOS (Non-Line of Sight) channel propagation condition. On the contrary, LOS (Line of Sight) condition is that the signal is not obstructed by the obstacle during the propagation. As shown in the Fig. 1, AN stands for AP and TN stands for signal receiving point. LOS condition is that the propagation of signals between AN and TN and there is no obstacle between the two points. The signal propagation between AN4 and TN is NLOS condition. Due to some block such as wall, door, other building structures, and human activities, signal propagation is often reflected, diffracted, and obscured, therefore, NLOS condition is ubiquitous.

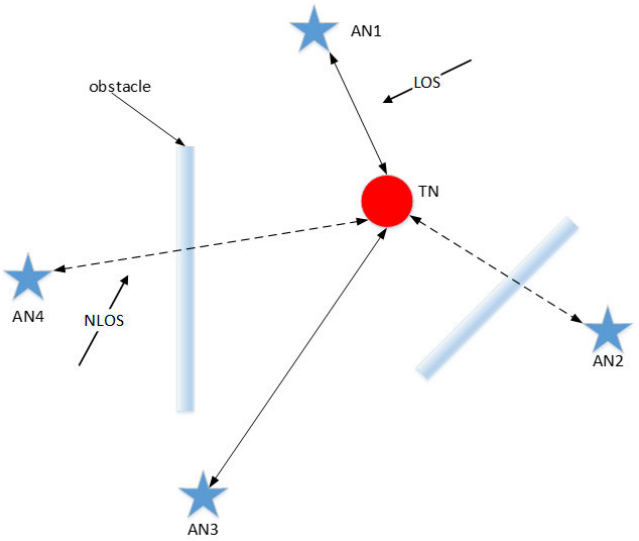

FIGURE 1. The illustration of LOS and NLOS environments.

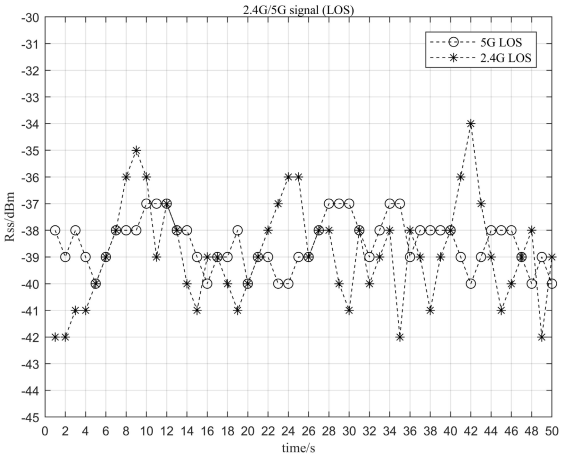

FIGURE 2. Signal performance of WiFi 2.4G and 5G in the LOS environment.

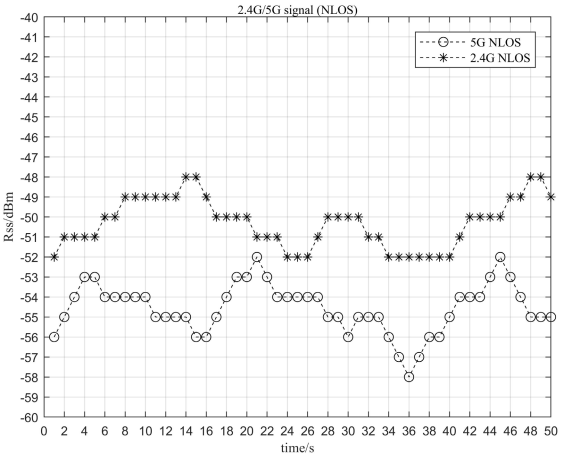

FIGURE 3. Signal performance of WiFi 2.4G and 5G in NLOS environment.

B. DUAL BANDS WiFi

2.4GHz and 5GHz are two main bands with the different frequency used for WiFi. Generally, the router we used can support both frequencies i.e 2.4GHz and 5GHz simultaneously. 2.4GHz though more widespread in usage (all 802.11b/g devices run on 2.4GHz only) has only 3 non-overlapping channels for transmission, which are crowded due to a lot of interfering devices, like other WiFi APs, microwave ovens, cordless phones, Bluetooth devices, etc [33]–[35]. All make for a noisy environment which increases interference and degrades the performance. On the other hand, the 5GHz channel is much cleaner with less interference with 23 non-overlapping channels, and 8 times more than 2.4GHz for transmission, which makes it suitable for applications like Video streaming and Gaming which are very sensitive to packet loss and delays. Normally, the WiFi 2.4G signal has higher coverage and penetrability but less speed. WiFi 5G has higher speed and stability but lesser penetrability [22]. Thus, because WiFi 2.4G does not attenuate much as the signal pass through obstacles such as walls and doors, we consider that WiFi 2.4G will have a better performance in the NLOS environments due to its high penetrability. On the contrary, the WiFi 5G signal is more suitable for the LOS environment by its higher stability.

The following data was collected to illustrate the stability condition between WiFi 2.4G/5G in NLOS/LOS conditions. To bring into correspondence with the signal performance, to collect data is adopted by Samsung cell phone. Staying in the room or separating by a wall is the way to receive LOS and NLOS signals. Figure 2 shows the RSS values of the WiFi 2.4G and 5G signal received from the fixed AP at the same location in the LOS condition. Fifty RSS values of WiFi 2.4G and 5G are collected at a 2 m distance with a frequency of 3s/time. Figure 3 evaluates the signal performance in the NLOS condition. To simulate the NLOS condition in our testing, the AP was put on the other room with one wall separation from the testing environment. The signal collection way is the same as the LOS condition. According to Fig. 2, the fluctuation of the WiFi 5G signal is smaller than the 2.4G signal in the LOS condition. The difference between the maximum RSS value and the minimum RSS value for the 5G signal is only three dBm, while for 2.4G signal, it is eight dBm. Besides, as shown in Fig. 3, the fluctuations between WiFi 2.4G and 5G are almost the same. However, the power difference of 2.4G is smaller than 5G. This indicates that the WiFi 2.4G signal has much higher penetrability than the 5G signal in the NLOS condition. Furthermore, the authors also collect values on five distinct and nearby positions to reveal the situations of WiFi signals. According to the results, the NLOS variance of WiFi 2.4G and WiFi 5G are 1.5612 and 1.5576 on the average, the average LOS variance of WiFi 2.4G and WiFi 5G are 3.6331 and 0.9078. These results also demonstrated the specific characters on WiFi 2.4G and WiFi 5G in different

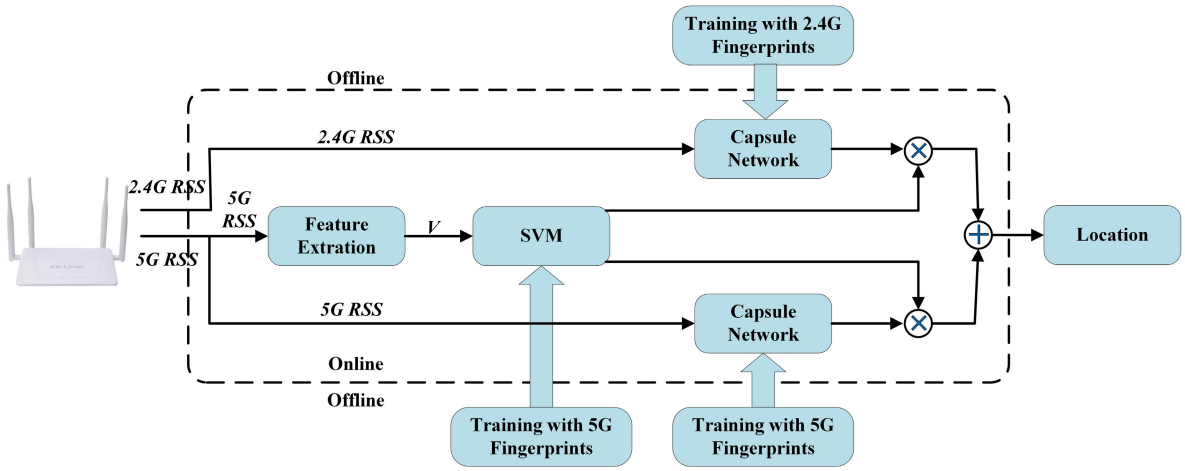

FIGURE 4. The system architecture.

environments. The signals of WiFi 2.4G and WiFi 5G are stable in the NLOS and LOS conditions respectively.

III. THE DESIGN OF BICN SYSTEM

A. SYSTEM OVERVIEW

In our study, based on the above descriptions, the WiFi 2.4G and 5G signal are employed as the input of our proposed BiCN system. That is, the characteristics of the WiFi dual bands are used to estimate the signal condition while the users stand indoors. Fig.4 illustrates the framework of the BiCN system. In the beginning, our system will create two offline fingerprinting databases in the same area, one is for the WiFi 2.4G signal, the other is for WiFi 5G. It's the offline part of our system. On the contrary, the procedure in the online phase is to estimate the user's position L^t at time t from a series of RSS values from all nearby APs, that is

$$L^t = F(r^t), \tag{1}$$

where r^t represents the collection of twenty RSS values of all nearby APs at fixed localization, including ten times of WiFi 2.4G signal and 5G signals. $F(.)$ is defined as the signal fuse learning method, which is the nonlinear mapping function to predict the user's location. In Fig.4, the process of $F(.)$ is divided into 3 parts, they are listed as follows,

- Features Extraction: For the purpose to increase the dimension of input vector, in our system, we extract four characteristics of mean, standard deviation, skewness and kurtosis from the series of RSS data $\tilde{r}_i$, expressed as $\tilde{v}_i = \{mean_{ij}^{2.4}, std_{ij}^{2.4}, skev_{ij}^{2.4}, kurt_{ij}^{2.4}, mean_{ij}^{5}, std_{ij}^{5}, skev_{ij}^{5}, kurt_{ij}^{5}, j = 1, 2, \ldots, K\}$. Note that, 2.4 and 5 in the upper-angled characteristics represent the data from WiFi 2.4G signal and WiFi 5G signal respectively. j indicates the jth AP.
- Fuse Learning Methods: In this part, we employed the SVM method to distinguish the WiFi signal state as NLOS or LOS condition, while the user stood indoor. According to our previous statement, the WiFi 5G signal has serious interference with the obstacles blocking. Thus, our fuse learning method is based on the training SVM model by the WiFi 5G signal. With the WiFi 5G signal help, we can obtain the probability to distinguish the signal condition of APs. This probability pass to the next part as the important degrees of WiFi 2.4G and 5G. On the other hand, we proposed two capsule networks trained by WiFi 2.4G and 5G fingerprint databases employed herein. Inputted with the WiFi 2.4G and 5G signals, these two capsule networks will derive the first position estimating results.
- Location Estimation: This part consists of the results of SVM and the capsule network. The result of SVM reveals the probability of the user's location in the NLOS or LOS condition. This value is mutual exclusive. Accordingly, the proposed capsule networks are used to obtain two estimating coordinates of WiFi 2.4G fingerprint and 5G fingerprint databases. Finally, the predicated position is combined with these results.

The following sections will introduce these parts sequentially.

B. FEATURES EXTRACTION

Accordingly, to better represent our system, every indoor area was regarded as the grid-based localization. The built fingerprint database is a $M \times (K + 1)$ matrix of M vectors $\{\tilde{l}_i, \tilde{r}_i, i = 1, 2, \ldots, M\}$, where M is the size of the database, and K is the numbers of APs. Each vector consists of a one-dimensional label $\tilde{l}_i$ of discrete position and the K-dimensional RSS vector, so the data of each position is the $(K + 1)$-dimensional vector. The RSS vector $\tilde{r}_i$ contains K elements $\tilde{r}_{ij}(j = 1, 2, \ldots, K)$, and each represents the observed RSS value of the jth AP.

As mentioned above, the WiFi 5G signal is obvious at the diagnosing of the conditions of NLOS and LOS. Thus, only the WiFi 5G signal is needed to extract the features as the input for the next stage. Each feature contains four values of mean, standard deviation, skewness, and kurtosis. Mean value refers to the average of all RSSs of an AP collected at one location. The value of standard deviation (std) and

skewness are derived as the same definition. Skewness is used to measure the asymmetry of the probability distribution. The formula to calculate the skewness is as follows:

$$skew_{ij} = \frac{\frac{1}{n}\sum_{k=1}^{n}(\tilde{r}_{ijk} - mean)^3}{(\frac{1}{n}\sum_{k=1}^{n}(\tilde{r}_{ijk} - mean)^2)^{\frac{3}{2}}}, \quad (2)$$

where $skew_{ij}$ represents the skewness feature of the jth AP at the ith position, and $\tilde{r}_{ijk}$ represents the kth RSS received by the jth AP at the ith position. n is the collecting numbers of RSS values. The *mean* represents the average of the data.

On the other hand, Kurtosis is used to describe the peak-to-peak characterizing values of the probability density distribution curve at averaging. Kurtosis expressed as (3).

$$kurt_{ij} = \frac{\frac{1}{n}\sum_{k=1}^{n}(\tilde{r}_{ijk} - mean)^4}{(\frac{1}{n}\sum_{k=1}^{n}(\tilde{r}_{ijk} - mean)^2)^2} - 3, \quad (3)$$

where $kurt_{ij}$ represents the kurtosis feature of the jth AP at the ith position.

C. FUSE LEARNING METHODS

1) SVM MODEL FOR THE NLOS AND LOS CONDITIONS

After extracting the WiFi 5G features, we employed the SVM model to distinguish the user located at the NLOS or LOS conditions, and this value is mutual exclusive in one. Besides, the collection of AP data is independent and identically distributed; the environment inference still causes the value mutually independent. For each AP, the corresponding SVM model is trained separately. For example, given a set of M training items $\{\tilde{v}_{ij}^5, b_{ij}, i = 1, 2, \ldots, M\}$, where $\tilde{v}_{ij}^5 = \{mean_{ij}^5, std_{ij}^5, skev_{ij}^5, kurt_{ij}^5\}$ is the ith reference point's fingerprinting consisting of a subset of features, $b_{ij} \in \{-1, 1\}$ indicates the ith reference point is in the NLOS/LOS condition towards the jth AP($b_{ij} = 1$ is LOS and $b_{ij} = -1$ is NLOS). Accordingly, the deriving example of each AP (jth AP) is listed as follows,

First, the optimal hyperplane of SVM model is defined as $w^T x + w_0 = 0$. This hyperplane satisfies the following condition; for the ith reference point, when $b_{ij} = 1, f(\tilde{v}_{ij}^5)$ is always greater than 0; when $b_{ij} = -1, f(\tilde{v}_{ij}^5)$ is always less than 0. Thus,

$$f(x) = w^T x + w_0. \quad (4)$$

In order to find this hyperplane, we need to maximize the geometry of the point closest to the plane, which is represented as $\frac{2}{\|w\|}$ in mathematics. In other words, to make the maximization of geometry, what we only need is to minimize $\|w\|$. This leads to a convex optimization problem. Then we use the Lagrange duality method to solve the convex problem. Lastly, we find the parameters w, w_0 that minimizes $\|w\|$ by (5).

$$\arg\min_{w,w_0} \frac{\|w\|^2}{2} + c\frac{1}{2}\sum_{i=1}^{M} e_i^2, e_i = 1 - b_{ij}(w^T \varphi(\tilde{v}_{ij}^5) + w_0), \quad \forall i \quad (5)$$

where w, w_0 are weight parameters learned from the training data using the above optimization, c is a custom weight coefficient and φ is the predetermined feature mapping function, which can map the feature vector to higher dimensional spaces. We use a Gaussian radial basis function (RBF) as our mapping function, that is

$$k(v_{mj}^5, \tilde{v}_{ij}^5) = \varphi(v_{mj}^5)^T \cdot \varphi(\tilde{v}_{ij}^5) = exp(-\frac{\|v_{mj}^5 - \tilde{v}_{ij}^5\|_2^2}{2\sigma^2}). \quad (6)$$

After (5), we find the optimal hyperplane and obtain the parameters w, w_0. These parameters can substitute into (4), and yield the result like (7),

$$f(x) = \sum_{i=1}^{M} \lambda_i b_{ij} k(x, \tilde{v}_{ij}^5) + w_0, \quad (7)$$

where λ_i is the Lagrange multiplier, and $k(x, \tilde{v}_{ij}^5)$ is the kernel function presented in (6). We define $h(x) = \sum_{i=1}^{M} \lambda_i b_{ij} k(x, \tilde{v}_{ij}^5)$, then $f(x)$ can be simplified as follow,

$$f(x) = h(x) + w_0. \quad (8)$$

Accordingly, the SVM method outputs the classification results directly. For the purpose to obtain the categorizing probability, we refer to Plat's method in [22], (9) is the output of posterior probability,

$$P(y = 1 \mid x) \approx P_{AB}(f) \equiv \frac{1}{1 + exp(Af + B)}, \quad (9)$$

where x is the feature vector of test point and y is the mathematical symbol describing the state of the test point. $P(y = 1 \mid x)$ represents the posterior probability. $P_{AB}(.)$ is a function of $f(x)$, which is the output result of the trained SVM model. A, B are the fitted parameters. The sigmoid function can well convert the output value of the SVM to the interval of (0,1), which is exactly the approximate range of probability. In fact, if we obtain the best parameters A and B, we can use (9) to discriminate whether the test point is in LOS or NLOS environment. For example, for the mth test point, its feature vector denotes as v_{mj}^5, its state for the jth denotes as b_{mj}. We substitute it into (9), and the probability of the jth AP in the LOS condition is listed as follow,

$$P(b_{ij} = 1 \mid v_{mj}^5) \approx P_{AB}(f) \equiv \frac{1}{1 + exp(Af + B)} \quad (10)$$

To find the optimum parameters, we minimize the negative logarithmic likelihood function of training data as shown in (11),

$$\arg\min_{A,B} -\sum_{i=1}^{N}(t_{ij}\log(p_{ij}) + (1 - t_{ij})\log(1 - p_{ij})), \quad (11)$$

where $p_{ij} = \frac{1}{1+exp(Af(v_{ij}^5+B)}$ denotes the probability that ith reference point is in the LOS environment for the jth AP calculate by (10). Furthermore, the probability of NLOS is $1 - p_{ij}$.

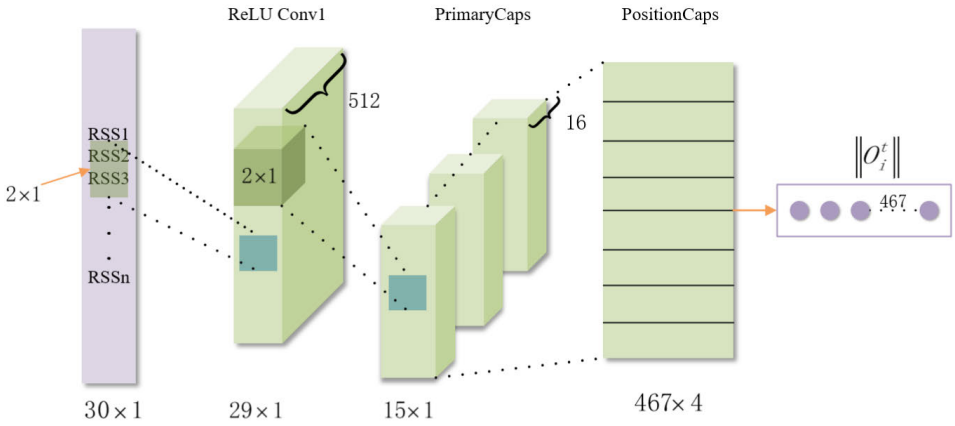

FIGURE 5. The system architecture.

2) THE CAPSULE NETWORK FOR THE ESTIMATION COORDINATION

The capsule neural network was proposed by Hinton, the proponent of the convolutional neural network, in 2017 [32]. In terms of image processing, the amount of training data required is much smaller than that of CNN, but the effect is not inferior to CNN, which is the advantage of the capsule network. In our study, we found that capsule network is also very capable of handling low-dimensional data. Thus, our system employed two capsule networks to calculate position coordinates, the specific structure of a single capsule network is shown in Fig.5. Our network model has four layers, there are the input, convolution, capsule, and fully connected layers. The input layer has a $10K$ dimensions. Taking a 2.4G network as an example, the input vector can be expressed as $\tilde{r}_{ij}$ $(j = 1, 2, \ldots, K)$, note that i is the number of the location, j is the jth AP in the total K APs. According to our design, the network input is a series of RSS values, not the preprocessed data, because the second layer of the convolution layer is designed for the feature extraction. That is, this layer can refine the feature of the RSS inputs, extend the local features, and refine the global feature for capsule network. The final purpose is we want to purify the original input. The third layer is the capsule layer and similar to the convolution layer. The difference is that the object involved in the convolution operation is no longer a single neuron, but a larger-sized neural capsule. A neural capsule can regard as a set of packed neurons to extract multiple features from the incoming data, then output a high-dimensional vector. About the fourth layer, it's fully connected and different from the ordinary neural network. The import reason is that the weight of the connection changed during the learning process. That is called the dynamic routing to strengthen the connection between the nodes. The output of the fourth layer is probabilities O^t, it is the predicted position at a possible position, and $O^t = \{O_i^t, i = 1, \ldots, M\}$. Finally, the position coordinate X with the highest probability is chosen as the predicted one. In order to ensure that the length of the output vector in the fully connected layer can better represent the probability of the position, a function is needed to map the length to the $[0 \sim 1)$ interval, and to ensure that the vector contains the same information. This function is called non-linear ''squashing'' function. The dynamic routing and non-linear ''squashing'' function will be introduced as follows,

About the dynamic routing in our system, the coupling strength of the lower layer capsule and the high layer capsule is controlled by the coupling coefficient C_{ij}, and we defined that $\sum_j C_{ij} = 1$, i indicates that the ith capsule in lower level, j represents the jth high-level active capsule to the one attached. In our study, the lower layer capsule refers to the third layer, and the high layer capsule refers to the last layer of the fully connected layer in the network. Besides, a flexible and orderly dynamic routing mechanism ensures that the useful information in the lower level capsule can send to the appropriate high-level capsule nodes. This definition is quite different from the traditional neural network. The traditional neural network sends all the information of the previous layer to the following layer, and the capsule network transmits the information to the next layer with emphasis. The weighted connection process of high-low-level nerve capsule is shown in the Fig.6.

Accordingly, the length of the output vector of a capsule is used to represent the probability. Therefore, using a non-linear ''squashing'' function can guarantee the short vectors shrinking to the almost zero length, and the long vectors shrinking to the length slightly. The function is shown in (12). Therefore, we leave it to discriminative learning to make good use of this non-linearity. That is,

$$v_j = \frac{\|s_j\|^2}{1 + \|s_j\|^2} \cdot \frac{s_j}{\|s_j\|}, \tag{12}$$

where v_j is the vector output of capsule j, and s_j is its total input. Furthermore, for all but the first layer in our network, the total input to a capsule s_j is a weighted sum over all ''prediction vectors'' $\widehat{u}_{j|i}$ from the capsules in the layer below and is produced by multiplying the output u_i of a capsule in

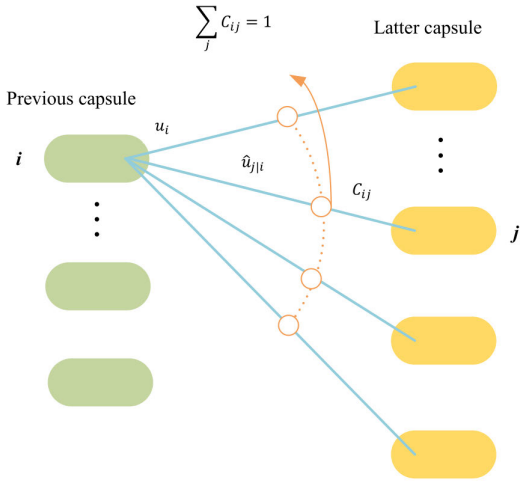

FIGURE 6. High-low-level nerve capsule connection diagram.

the layer below by a weight matrix W_{ij}.

$$s_j = \sum_i C_{ij}\widehat{u}_{j|i}, \widehat{u}_{j|i} = W_{ij}u_i, \tag{13}$$

where C_{ij} is the coupling coefficient determined by the iterative dynamic routing process. Besides, the coupling coefficients between capsule i and all the capsules in the layer above are summarized to one, and these coupling coefficients are computed by a ''routing softmax''. The initial logits b_{ij} of ''routing softmax'' are the log prior probabilities and the capsule i should be coupled to capsule j. The description of the coupling coefficient is listed as follows,

$$C_{ij} = \frac{exp(b_{ij})}{\sum_k exp(b_{ik})}. \tag{14}$$

Moreover, the log priors can be learned at the same time for all the other weights discriminatively. The initial coupling coefficients are iteratively refined by measuring the agreement between the current output v_j of each capsule j and the prediction $\widehat{u}_{j|i}$ made by capsule i. Finally, the agreement is treated as if it was a log likelihood and is added to the initial logit b_{ij}.

Thus, the length of the instantiation vector represents the probability of a capsule's entity exists. The top-level capsule for digit class k has a long instantiation vector if and only if that digit is present in the image. To allow for multiple digits, our system uses a separate margin loss, L_k for each digit capsule k, that is

$$L_k = T_k max(0, m^+ - \|v_K\|)^2 + \lambda(1-T_k)max(0, \|v_k\| - m^-)^2, \tag{15}$$

where $T_k = 1$ iff a position of class k is existed and $m^+ = 0.9$ and $m^- = 0.1$. The λ will stop the initial learning from shrinking the lengths of the activity vectors, and can downweight of the loss for absent position classes. In our study, we defined $\lambda = 0.5$ as our experiences.

Algorithm 1 Dynamic Routing

1: procedure ROUTING($(\widehat{u}_{j|i})$, r, l)
2: **for** all capsule i in layer l and capsule j in layer $(l+1)$: $b_{ij} \leftarrow 0$.
3: **for** r iterations **do**
4: **for** all capsule i in layer l: $C_i \leftarrow$ softmax(b_i) ▷ softmax computes (14)
5: **for** all capsule j in layer $(l+1)$: $s_j \leftarrow \sum_i C_{ij}\widehat{u}_{j|i}$
6: **for** all capsule j in layer $(l+1)$: $v_j \leftarrow$ squash(s_j) ▷ softmax computes (12)
7: **for** all capsule i in layer l and capsule j in layer $(l+1)$: $b_{ij} \leftarrow b_{ij} + \widehat{u}_{j|i} \cdot v_j$
8: **end for**
9: **return** v_j

D. LOCATION ESTIMATION

According to the above description, when a user wants to predict his location, then his smartphone will receive a series of RSS values. Then, our proposed SVM method is used to derive the probabilities of NLOS/LOS condition by the signal received from each AP in the current position. At the same time, these RSS values pass to the capsule network to obtain the predicted coordinates. Finally, the final position is obtained through the weight computation of (16) and (17). According to our assumption, our system is based on the derivation of the WiFi 2.4G/5G signals. For the location estimation in the same place, the derived probabilities are added as the total confidence for WiFi 2.4G, and WiFi 5G, the equations are listed as follows,

$$W_i^N = \sum_{j=1}^{K} w_{ij}^N, \tag{16}$$

and

$$W_i^L = \sum_{j=1}^{K} w_{ij}^L, \tag{17}$$

where W_i^N and W_i^L represent the sum of the probabilities that all signal states at the ith position are in NLOS and LOS conditions, w_{ij}^N and w_{ij}^L are defined as the probability that the signal transmitted by the jth AP in the ith position is in the NLOS and LOS condition either. Finally, in the positioning step, the position coordinates are calculated from the network trained by the 2.4G signal can be expressed as $X_t^{2.4}$, and 5G as X_t^5, for $t = 1, 2, ...$ The final position coordinate is obtained by multiplying of their respectively total confidences. The formula is listed as follows,

$$L = \frac{W_i^N}{W_i^N + W_i^L} X_t^{2.4} + \frac{W_i^L}{W_i^N + W_i^L} X_t^5. \tag{18}$$

IV. EXPERIMENTS AND DISCUSSION

A. EXPERIMENT ENVIRONMENT INITIALIZATION

In our experiment environment, we conducted a complex indoor environment on the first floor of the 55th office

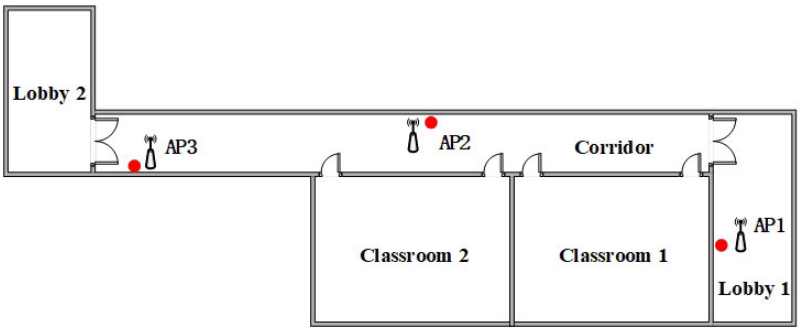

FIGURE 7. Physical field environment.

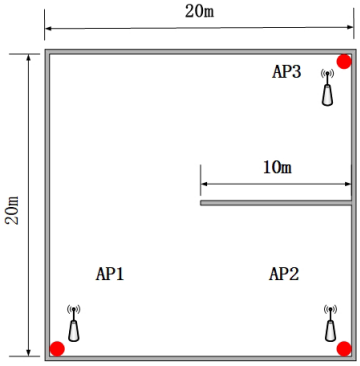

FIGURE 8. Simulating environment.

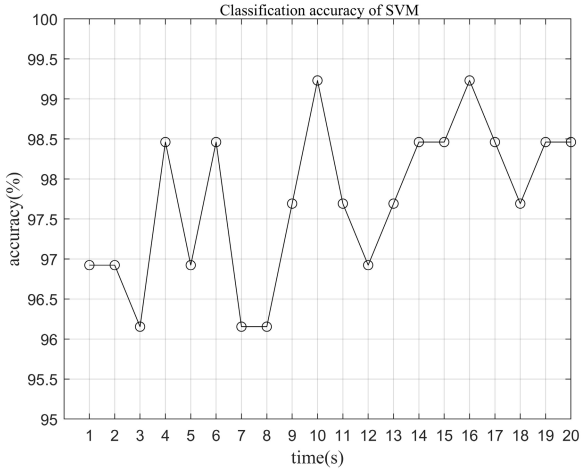

FIGURE 9. Accuracy rates of NLOS state discrimination.

building of Tianjin University, including two halls, one corridor, and two classrooms. The area was approximately 12 m×16 m for the classrooms 1 and 2. Every classroom divided into 63 rectangular squares with an area of 1.2 m×1.2 m. The area of the corridor was about 50 m×50 m, and the area of the first and second halls were 12.3 m×6.6 m and 13.6 m×7 m respectively. People were free to walk around in these areas. To receive the online RSS data, the Samsung cell phone (Note S9) was used as the data collector in the testing areas, according to our previous studies, the antenna design of Samsung cell phones was much more stable than the other brands at the data collection. Accordingly, we use three Tenda AC9 routers in our experiments which support both WiFi 2.4G and 5G frequency bands. For each AP, twenty RSS values were collected at the fixed positions for each AP as our offline fingerprint database. Note that these areas contain many NLOS inference factors, like obstacles, doors, walls and human activities. Figure 7 is the illustration of our physical testing area. On the other hand, to test our system in the diversity area, we also carried out the simulation testing area as the wide-range experiment environment. This environment was assumed in a 20 m×20 m square space by MATLAB R2017b. The whole environment was divided into 400 small pieces with a square area of 1 m×1 m. These places exist several walls and doors, please review Fig.8 for the detail.

B. DISCRIMINATION ON NLOS CONDITION

For the purpose to check the discrimination on NLOS condition, in this experiment, the eigenvector of the 5G signal of the test point in our physic area substituted into (10) and (11) to obtain the prediction of NLOS condition. Total twenty experiments were employed to illustrate the accuracy of the discrimination. According to Fig.9, the minimum accuracy rate of the discrimination is no less than 96%, most of the accuracies are higher than 97%. This result indicates that our method has an outstanding in the discrimination on NLOS condition. Besides, this result also indicates the WiFi 5G signal is more suitable for the discrimination due to its significant differences between LOS and NLOS environment.

C. LOCATION ESTIMATION IN THE PHYSICAL FIELD ENVIRONMENT

In this experiment, we want to test the performance of location estimation in the physical field environment with several different methods, including our proposed method, KNN [36], WKNN [21], Cluster KNN [22], and DGPR proposed by Fei Teng [26]. In the traditional indoor position system, KNN, WKNN and Cluster KNN were proposed to categorize the fingerprint database into a small group, then a user can derive his position in this small group easily. On the other hand, DGPR is a nonparametric model in the indoor position system, and this model only needs to measure part of the reference points for the future usage, thus reducing the

TABLE 1. Performances of different methods in the field experiment.

Methods	Average Error(m)	1 m	2 m	3 m	5 m
KNN	2.40	17.81%	47.95%	65.75%	95.89%
WKNN	1.86	32.39%	64.79%	83.09%	98.59%
Cluster KNN	2.09	26.02%	58.90%	76.71%	93.15%
DGPR	2.38	14.54%	52.73%	69.09%	94.55%
CN2.4G	1.13	64.38%	80.82%	89.04%	98.63%
CN5G	1.11	65.75%	82.19%	90.41%	98.63%
BiCN	0.99	58.82%	88.23%	95.59%	100%

time and cost required for data collection. In this experiment, we tried to reveal our outstanding performance by comparing with three traditional fingerprint models and one learning model. Accordingly, we compared the estimation accuracy in Table 1 and plotted the CDF (cumulative distribution function) of different methods in Fig.10. In Table 1, the average localization errors are 2.40 m, 1.86 m, 2.09 m and 2.38 m, respectively. Our proposed methods with CN2.4G (trained and tested by WiFi 2.4G data), CN5G (trained and tested by WiFi 5G data) and BiCN have the average errors with 1.13 m, 1.11 m and 0.99 m. Obviously, our proposed methods have better positioning accuracy. Furthermore in Table 1, about the three methods using the capsule network, all over 50% of the test positions have an error smaller than 1 m. The other methods of KNN, WKNN, Cluster KNN and DGPR with a positioning error under one meter are less than 50%. Thus it can be seen the superior performance of the capsule network. Moreover, in Table 1, we observe that the positioning error of the network trained with WiFi 5G alone is better than the positioning error of trained with WiFi 2.4G. In Fig.10, we also found our proposed BiCN method using with WiFi 2.4G and WiFi 5G to locate the position can speed up the convergence. There is a very small difference of positioning error under 1 m among using CN2.4G, CN5G and BiCN. On the contrary, in the range of 2 m to 4 m, the CDF of error proportion by BiCN is higher than that of CN2.4G and CN5G. The reason is that when the received signal is in the NLOS condition, the method will trust the WiFi 2.4G signal more with greater confidence, and vice versa with WiFi 5G in LOS condition. This switch step can increase the system flexibility during the learning process. Generally, the position methods mentioned above consisted of two parts, the offline training part, and online testing part, please refer to Fig.4. The offline training system is the data collection phase. To face user requirement is the process of online system. According to our test in the field environment, the execution time of KNN, WKNN, Cluster KNN, DGPR, CN2.4G, CN5G, and BiCN are 0.45 s, 0.56 s, 1.17 s, 0.54 s, 0.72 s, 0.72 s, and 0.85 s respectively. Through our field testing, the execution time of less than one second is tolerable. Although the execution time is higher, the more accuracy rate is much better than others.

D. LOCATION ESTIMATION IN THE SIMULATING ENVIRONMENT

In order to simulate the environment with different noise, we referred the logarithmic distance model to generate

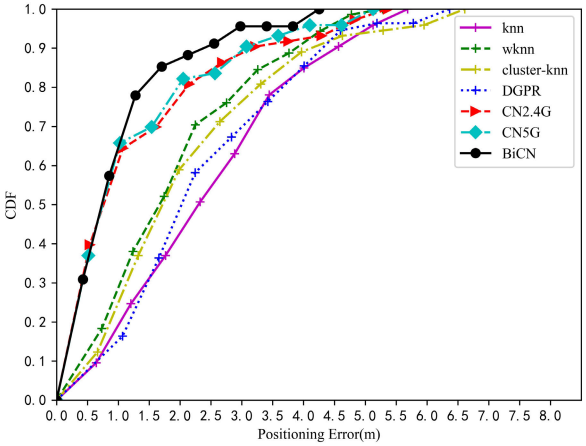

FIGURE 10. CDF plot of different methods in the field environment.

TABLE 2. Common empirical value of attenuation factor.

Environment	N
office	1.4-2.5
corridor	1.9-2.5
park	2.7-3.4
lawn	3.0-3.9
sand beach	3.8-4.6

simulation data, that is

$$P(d)_{dBm} = P(d_0)_{dBm} - 10 \times N \times \log\left(\frac{d}{d_0}\right) - X_\delta, \quad (19)$$

where N indicates the rate of increase in the signal attenuation with the propagation distance, $P(d_0)$ is the RSS at a distance of reference point d_0, and d is the distance between the transmitter and the receiver [37]. Furthermore, N is the attenuation factor, and X_δ is the noise generated by the Gaussian random distribution that standard deviation is δ and mean is 0. We use X_δ to represent the effects of obstacles on the RSS. According to our experiences, the attenuation factor N of the logarithmic distance model has a great relationship with the surrounding environment. In [38]–[40], the empirical values of N in different environments are summarized as Table 3. N is assumed as 2 to approximate to our collected data in the field environment. Besides, we simulate the WiFi 2.4G and 5G signals by the following two characteristics; one is the decay of WiFi 2.4G less influenced by the objects blocking and vice versa. Comparing Fig. 2 and Fig. 3, the average attenuation of WiFi 2.4G and 5G are eleven dBm and sixteen dBm, respectively. These values are defined as different Ns to represent the WiFi 2.4G and 5G signal in Eq. 19. The second characteristic is that the fluctuation of WiFi 2.4G signal is excellent than the WiFi 5G signal. Therefore, noise mappings are different for WiFi 2.4G and 5G.

Like the previous experiment, we test the performance of location estimation in the stimulating environment with our proposed method, KNN, WKNN, Cluster KNN, and DGPR. In this simulating area, it's the 20 m×20 m square divided by 400 pieces of small 1 m×1 m area (Fig.8).

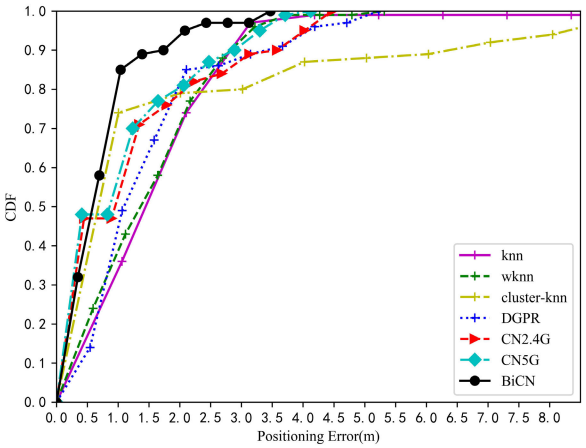

FIGURE 11. CDF plot of different methods in the simulate environment.

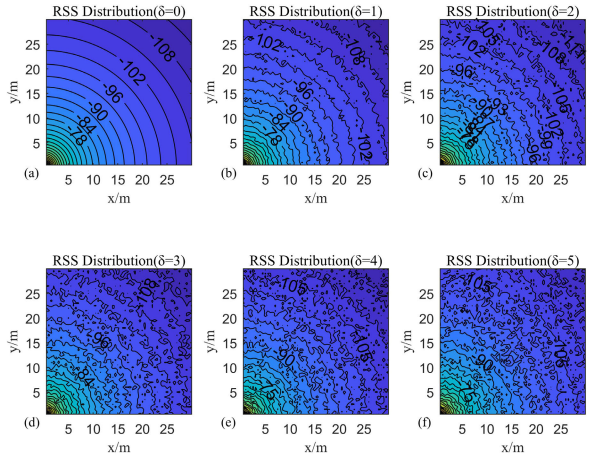

FIGURE 12. Received signal strength(RSS) strength mapping with different noise: (a) $\delta = 0$; (b) $\delta = 1$; (c) $\delta = 2$; (d) $\delta = 3$; (e) $\delta = 4$; (f) $\delta = 5$.

These places exist several walls and doors, and we equipped three APs in the top right, left the bottom and lower right corner corners. Figure11 shows the CDF of location errors of the seven methods. Generally, in this complex propagation environment, with the BiCN method help, 100% of the test positions have an error smaller than 5 m, while KNN, WKNN, Cluster KNN, and DGPR achieved an error of less than 5 m approximately as 99.17%, 99.17%, 88.33%, and 97.50% of the test locations, respectively. Besides, the error rate in 1 m, we can see that the percentage of test positions are 84.17%,48.33%,74.17%,38.33% and 32.89% for BiCN, DGPR, Cluster KNN, WKNN, and KNN, respectively. These results still reveal the advantage of our proposed method.

TABLE 3. Performances of different methods in the simulate experiment.

Methods	Average Error(m)	1 m	2 m	3 m	5 m
KNN	1.54	32.89%	72.39%	93.83%	99.17%
WKNN	1.46	38.33%	74,17%	95.83%	99.17%
Cluster KNN	1.34	74.17%	79.17%	80.00%	88.33%
DGPR	1.47	48.33%	80.00%	88.33%	97.50%
CN2.4G	1.05	70.83%	81.67%	91.66%	100%
CN5G	0.96	70.00%	82.19%	90.41%	100%
BiCN	0.76	84.17%	95.00%	97.50%	100%

E. THE ROBUSTNESS FOR LOCALIZATION ACCURACY

In this experiment, we wanted to verify the robustness of the proposed method. Thus, the environmental changes was simulated in the same area by setting different δ values in (19). That is, the larger the standard deviation of the noise term of X_δ, the greater the effect on signal propagation. As we can see in Fig. 12(a), this figure consists of different arcs, each arc represents the same RSS value but different coordinates in an area. Moreover, Figures 12(b)-(f) show the RSS mappings with δ equaling 1, 2, 3, 4, 5 for the noise term of X_δ. The origin of the coordinate axis is the location of the AP. In the ideal case, the RSS values strictly fit the log model and there does not exist of the signal interference. As long as the reference points keep the same distance from that AP, the receiver in these reference points will obtain the same RSS values. This situation is shown in Fig. 12(a). When the environmental noise and the RSS fluctuation are getting worse and worse, the interference of RSS values is shown in Fig. 12(b)-(f) respectively. For example, Figure 12(b) illustrates the small differences of RSS values with the same distance from the AP, this situation represents the slightly environmental changes. Figures 12(a) and 12(b) are very similar. Furthermore, the increasing of environmental noise δ values will confuse the stable of the RSS values.

TABLE 4. Common empirical value of attenuation factor.

ID of environment	2.4G training/testing	5G training/testing
E1(General Area)	1/1	0.5/0.5
E2(Light Crowds Area)	1/2	0.5/1
E3(Median Crowds Area)	1/3	0.5/1.5
E4(Heavy Crowds Area)	1/4	0.5/2
E5(Super Heavy Crowds Area)	1/5	0.5/2.5

To evaluate the robustness of our proposed algorithm, we simulated five different environments in Table 4. These attenuation factors of testing and training areas were indicated as the five crowding degrees of normal (represented as E1), light (E2), medium (E3), heavy (E4) and super heavy (E5) in WiFi 2.4G and 5G environments. The numbers of humans can be represented as the interference of the signal. We trained our model on the normal situation and tested on the specific crowds in the same area. Thus, in Table 4, the training and testing attenuation factors are 1 and 1, 1 and 2, 1 and 3, 1 and 4, 1 and 5, respectively in E1, E2, E3, E4 and E5 with WiFi 2.4G. Furthermore, the training and testing attenuation factors are 0.5 and 0.5, 0.5 and 1, 0.5 and 1.5, 0.5 and 2, 0.5 and 2.5, respectively in E1, E2, E3, E4 and E5 with WiFi 5G.

In the environments E2-E5, the localization errors were compared in Fig. 13(a)-13(d). We can see that the robustness

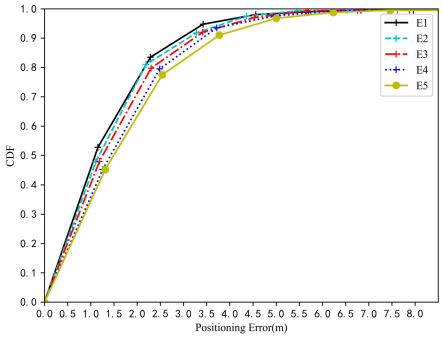

(a)

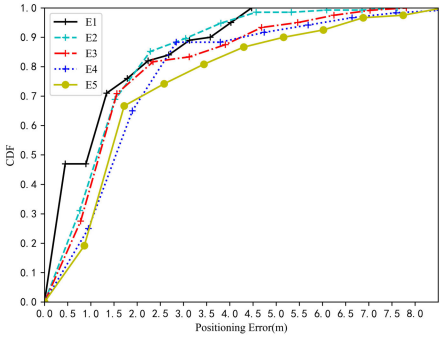

(b)

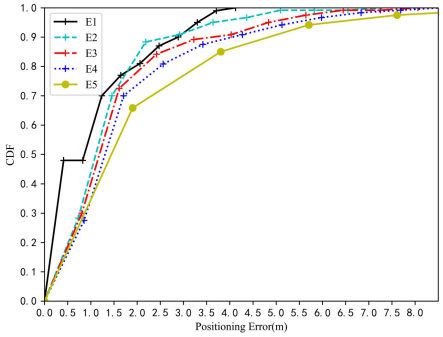

(c)

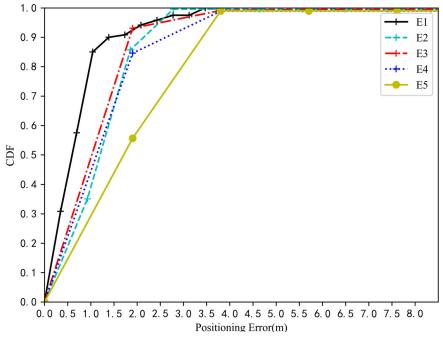

(d)

FIGURE 13. CDF of simulated localization error for different noisy environments: (a) the DGPR method; (b) the CN2.4G method; (c) the CN5G method; (d) the BiCN method.

of the DGPR is better. The mean positioning error of our method has a slight fluctuation in the environment with a different noise, which is 0.76 m, 0.84 m, 0.87 m, 1.15 m and 1.54 m. The positioning error of DGPR is 1.39 m, 1.45 m, 1.55 m, 1.72 m, and 1.83 m in the E5. As shown in Table 5, BiCN still has a mean localization error within 1 m in the first three environments and its mean positioning error is 1.54 m in the E5 where the noise is largest. The CN2.4G and CN5G are slightly worse, which mean error is 1.92 m and 1.89 m respectively. The DGPR method is better than CN2.4G and CN5G, which mean positioning error is 1.83 m in the E5. In summary, our method has strong robustness and can achieve higher positioning accuracy even when strong interference is encountered.

TABLE 5. Localization error of four different methods in five different environments.

method	E1	E2	E3	E4	E5
DGPR	1.39	1.45	1.55	1.72	1.83
CN2.4G	1.05	1.28	1.50	1.56	1.92
CN5G	0.96	1.23	1.37	1.53	1.89
BiCN	0.76	0.84	0.87	1.15	1.54

V. CONCLUSION

Nowadays, internet technology is developing rapidly, WiFi networks are becoming more and more popular, and its coverage is becoming wider and wider. Therefore, WiFi-based indoor positioning technology has become more and more popular due to its simplicity, low cost. Thus, many commercial applications for indoor positioning are based on WiFi. In our study, the bi-modal with 2.4GHz and 5GHz and a deep learning system for fingerprinting-based indoor localization are proposed as BiCN. That is, the characteristics of the WiFi dual bands are used to estimate the signal condition while the users stand indoors. First, our system will create two offline fingerprinting databases in the same area, one is for the WiFi 2.4G signals, the other is for WiFi 5G. Two characteristics of the dual bands are referred in our study, one is the decay of the WiFi 2.4G signal is less influenced by the objects blocking, on the contrary, WiFi 5G is seriously worse than WiFi 2.4G. The second characteristic is that the fluctuation of the WiFi 2.4G signal is great than the WiFi 5G signal. Thus, the procedure in the online phase is to estimate the user's position by the proposed features extraction and fuse learning methods. The main focus in feature extraction is based on the obviousness at WiFi 5G at the diagnosing of the condition of NLOS and LOS. Thus, four values of mean, standard deviation, skewness, and kurtosis are derived from the received signals. Accordingly, we employed the SVM model to weight the chance of the user located at the NLOS or LOS environment, and the capsule networks are also employed to calculate position coordinates.

Comparing with traditional positioning methods, those methods took time on the designing algorithm for fitting heterogeneous signals, filtering results and tuning parameters on the non-linear model. Our proposed BiCN can utilize the WiFi dual bands' signal as the tool to recognize the LOS and NLOS situations, learn the mapping structure between ground-truth positions and fingerprinting database. Because

of the adaptive and efficiency of the BiCN, the proposed positioning scheme achieves excellent positioning ability with high accuracies. The experimental results validated the performance of BiCN over several benchmark schemes.

REFERENCES

[1] L. Li, Y. Wang, X. Ma, C. Chen, and X. Guan, "Dual-tone radio interferometric positioning systems for multi-target localization using a single mobile anchor," *China Commun.*, vol. 12, no. 1, pp. 25–35, Jan. 2015.

[2] J.-W. Steeb, D. B. Davidson, and S. J. Wijnholds, "Computationally efficient radio frequency source localization for radio interferometric arrays," *Radio Sci.*, vol. 53, no. 3, pp. 242–256, Mar. 2018.

[3] C. Lee, Y. Chang, G. Park, J. Ryu, S.-G. Jeong, S. Park, J. W. Park, H. C. Lee, K.-S. Hong, and M. H. Lee, "Indoor positioning system based on incident angles of infrared emitters," in *Proc. 30th Annu. Conf. IEEE Ind. Electron. Soc. (IECON)*, vol. 3, Nov. 2004, pp. 2218–2222.

[4] G. Retscher, V. Gikas, H. Hofer, H. Perakis, and A. Kealy, "Range validation of uwb and wi-fi for integrated indoor positioning," *Appl. Geomatics*, vol. 11, no. 2, pp. 187–195, Jun. 2019. doi: 10.1007/s12518-018-00252-5.

[5] X. Cai, L. Ye, and Q. Zhang, "Ensemble learning particle swarm optimization for real-time uwb indoor localization," *EURASIP J. Wireless Commun. Netw.*, vol. 2018, no. 1, p. 125, May 2018. doi: 10.1186/s13638-018-1135-0.

[6] G. Yong, Z. Cai, and H. Dong, "A high precision indoor cooperative localization scheme based on UWB signals," in *Wireless and Satellite Systems*, M. Jia, Q. Guo, and W. Meng, Eds. Cham, Switzerland: Springer, 2019, pp. 628–636.

[7] Y. Xu, Y. S. Shmaliy, Y. Li, and X. Chen, "UWB-based indoor human localization with time-delayed data using EFIR filtering," *IEEE Access*, vol. 5, pp. 16676–16683, 2017.

[8] Q. Shi, S. Zhao, X. Oui, M. Lu, and M. Jia, "Anchor self-localization algorithm based on UWB ranging and inertial measurements," *Tsinghua Sci. Technol.*, vol. 24, no. 6, pp. 728–737, Dec. 2019.

[9] H. Xie, T. Gu, X. Tao, H. Ye, and J. Lu, "A reliability-augmented particle filter for magnetic fingerprinting based indoor localization on smartphone," *IEEE Trans. Mobile Comput.*, vol. 15, no. 8, pp. 1877–1892, Aug. 2016.

[10] Y. Shu, C. Bo, G. Shen, C. Zhao, L. Li, and F. Zhao, "Magicol: Indoor localization using pervasive magnetic field and opportunistic WiFi sensing," *IEEE J. Sel. Areas Commun.*, vol. 33, no. 7, pp. 1443–1457, Jul. 2015.

[11] L. Fan, X. Kang, Q. Zheng, X. Zhang, X. Liu, C. Chen, and C. Kang, "A fast linear algorithm for magnetic dipole localization using total magnetic field gradient," *IEEE Sensors J.*, vol. 18, no. 3, pp. 1032–1038, Feb. 2018.

[12] S. Song, C. Hu, and M. Q.-H. Meng, "Multiple objects positioning and identification method based on magnetic localization system," *IEEE Trans. Magn.*, vol. 52, no. 10, Oct. 2016, Art. no. 9600204.

[13] C.-H. Ou, B.-Y. Wu, and L. Cai, "GPS-free vehicular localization system using roadside units with directional antennas," *J. Commun. Netw.*, vol. 21, no. 1, pp. 12–24, Feb. 2019.

[14] S. Kumar, "Performance analysis of RSS-based localization in wireless sensor networks," *Wireless Pers. Commun.*, vol. 108, pp. 769–783, Sep. 2019. doi: 10.1007/s11277-019-06428-5.

[15] L. Pei, J. Liu, Y. Chen, R. Chen, and L. Chen, "Evaluation of fingerprinting-based WiFi indoor localization coexisted with Bluetooth," *J. Global Positioning Syst.*, vol. 15, no. 1, p. 3, Oct. 2017. doi: 10.1186/s41445-017-0008-x.

[16] M. Zhou, M. Dolgov, Y. Liu, and Y. Wang, "WiFi/PDR integrated system for 3D indoor localization," in *Machine Learning and Intelligent Communications*, L. Meng and Y. Zhang, Eds. Cham, Switzerland: Springer, 2018, pp. 451–459.

[17] Z. Turgut, S. Üstebay, G. Z. G. Aydın, and A. Sertbaş, "Deep learning in indoor localization using WiFi," in *Proc. Int. Telecommun. Conf.*, A. Boyaci, A. R. Ekti, M. A. Aydin, and S. Yarkan, Eds. Singapore: Springer, 2019, pp. 101–110.

[18] Z. Yang and K. Järvinen, "Modeling privacy in WiFi fingerprinting indoor localization," in *Provable Security*, J. Baek, W. Susilo, and J. Kim, Eds. Cham, Switzerland: Springer, 2018, pp. 329–346.

[19] X. Lu, J. Wang, Z. Zhang, H. Bian, and E. Yang, "WiFi-based indoor positioning system with twice clustering and multi-user topology approximation algorithm," in *Geo-Spatial Knowledge and Intelligence*, H. Yuan, J. Geng, and F. Bian, Eds. Singapore: Springer, 2017, pp. 265–272.

[20] Q. Li, W. Li, W. Sun, J. Li, and Z. Liu, "Fingerprint and assistant nodes based Wi-Fi localization in complex indoor environment," *IEEE Access*, vol. 4, pp. 2993–3004, 2016.

[21] Z. Liu, X. Luo, and T. He, "Indoor positioning system based on the improved W-KNN algorithm," in *Proc. IEEE 2nd Adv. Inf. Technol., Electron. Automat. Control Conf. (IAEAC)*, Mar. 2017, pp. 1355–1359.

[22] F. Yu, M. Jiang, J. Liang, X. Qin, M. Hu, T. Peng, and X. Hu, "5G WiFi signal-based indoor localization system using cluster k-nearest neighbor algorithm," *Int. J. Distrib. Sensor Netw.*, vol. 10, no. 12, 2014, Art. no. 247525.

[23] A. Farshad, J. Li, M. K. Marina, and F. J. Garcia, "A microscopic look at WiFi fingerprinting for indoor mobile phone localization in diverse environments," in *Proc. Int. Conf. Indoor Positioning Indoor Navigation (IPIN)*, 2013, pp. 1–10.

[24] K. S. Kim, S. Lee, and K. Huang, "A scalable deep neural network architecture for multi-building and multi-floor indoor localization based on wi-fi fingerprinting," *Big Data Anal.*, vol. 3, no. 1, p. 4, Dec. 2018. doi: 10.1186/s41044-018-0031-2.

[25] C. Cai, L. Deng, M. Zheng, and S. Li, "PILC: Passive indoor localization based on convolutional neural networks," in *Proc. Ubiquitous Positioning, Indoor Navigation Location-Based Services (UPINLBS)*, Mar. 2018, pp. 1–6.

[26] F. Teng, W. Tao, and C.-M. Own, "Localization reliability improvement using deep Gaussian process regression model," *Sensors*, vol. 18, no. 12, p. 4164, 2018. [Online]. Available: https://www.mdpi.com/1424-8220/18/12/4164

[27] M. A. Landolsi, A. F. Almutairi, and M. A. Kourah, "LOS/NLOS channel identification for improved localization in wireless ultra-wideband networks," *Telecommun. Syst.*, pp. 1–16, Apr. 2019. doi: 10.1007/s11235-019-00572-w.

[28] Z. Xiao, H. Wen, A. Markham, N. Trigoni, P. Blunsom, and J. Frolik, "Non-line-of-sight identification and mitigation using received signal strength," *IEEE Trans. Wireless Commun.*, vol. 14, no. 3, pp. 1689–1702, Mar. 2015.

[29] X. Li, X. Cai, Y. Hei, and R. Yuan, "NLOS identification and mitigation based on channel state information for indoor WiFi localisation," *IET Commun.*, vol. 11, no. 4, pp. 531–537, Mar. 2017.

[30] Y. Zhang, W. Fu, D. Wei, J. Jiang, and B. Yang, "Moving target localization in indoor wireless sensor networks mixed with LOS/NLOS situations," *EURASIP J. Wireless Commun. Netw.*, vol. 2013, p. 291, Dec. 2013.

[31] K. Yu, K. Wen, Y. Li, S. Zhang, and K. Zhang, "A novel NLOS mitigation algorithm for UWB localization in harsh indoor environments," *IEEE Trans. Veh. Technol.*, vol. 68, no. 1, pp. 686–699, Jan. 2019.

[32] S. Sabour, N. Frosst, and G. E. Hinton, "Dynamic routing between capsules," in *Proc. Adv. Neural Inf. Process. Syst. (NIPS)*, vol. 30, 2017, pp. 1–11.

[33] L. Hong and Y.-W. Wu, "Path loss measurement of 2.4G band radio signal communication in disaster ruins," in *Proc. 16th Int. Symp. Commun. Inf. Technol. (ISCIT)*, 2016, pp. 439–444.

[34] M. Ayyash, H. Elgala, A. Khreishah, V. Jungnickel, T. Little, S. Shao, M. Rahaim, D. Schulz, J. Hilt, and R. Freund, "Coexistence of WiFi and LiFi toward 5G: Concepts, opportunities, and challenges," *IEEE Commun. Mag.*, vol. 54, no. 2, pp. 64–71, Feb. 2016.

[35] H. Xiong, X. Zhu, and R. Zhang, "Energy recovery strategy numerical simulation for dual axle drive pure electric vehicle based on motor loss model and big data calculation," *Complexity*, vol. 2018, pp. 1–14, Aug. 2018, Art. no. 4071743. doi: 10.1155/2018/4071743.

[36] Y. Xie, Y. Wang, A. Nallanathan, and L. Wang, "An improved K-nearest-neighbor indoor localization method based on spearman distance," *IEEE Signal Process. Lett.*, vol. 23, no. 3, pp. 351–355, Mar. 2016.

[37] X. Gan, B. Yu, L. Huang, and Y. Li, "Deep learning for weights training and indoor positioning using multi-sensor fingerprint," in *Proc. Int. Conf. Indoor Positioning Indoor Navigat. (IPIN)*, Sep. 2017, pp. 1–7.

[38] X. Wen, W. Tao, C.-M. Own, and Z. Pan, "On the dynamic RSS feedbacks of indoor fingerprinting databases for localization reliability improvement," *Sensors*, vol. 16, no. 8, p. 1278, Aug. 2016.

[39] S. Li, Z. Meng, and C.-M. Own, "The indoor NLOS identification on dempster-shafer evidence theory," in *Proc. ICCIP*, 2016, pp. 238–243.

[40] H. Wang, S. Sen, A. Elgohary, M. Farid, M. Youssef, and R. R. Choudhury, "No need to war-drive: Unsupervised indoor localization," in *Proc. MobiSys*, 2012, pp. 197–210.

CHUNG-MING OWN received the M.S. degree in information management from the National Yunlin University of Science and Technology, Taiwan, China, in 1998, and the Ph.D. degree from the Department of Computer Science and Information Engineering, National Chung Cheng University, Taiwan, in 2005.

From 2005 to 2013, he was an Associate Professor with the Department of Computer and Communication Engineering, St. John's University. In 2013, he was a Research Fellow with the School of Electrical and Computer Engineering, Georgia Institute of Technology, Atlanta, GA, USA. Since 2015, he has been holding the teaching position with the College of Intelligence and Computing, Tianjin University, China. His research interests include the development of augmented reality and intelligent medical treatment techniques using artificial intelligent methods, and indoor positioning methods in the IoT.

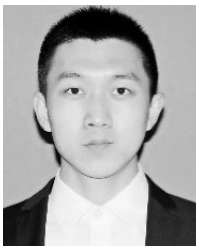

JIAWANG HOU was born in Liaoning, China, in 1994. He received the B.S. degree from the College of Aerospace Engineering, Shenyang Aerospace University, China, in 2017. He is currently pursuing the M.S. degree in software engineering with the College of Intelligence and Computing, Tianjin University. His research interests include virtual reality, augmented reality, classification, and the Internet of Things. He also focuses on indoor localization and deep learning.

WENYUAN TAO received the B.S. degree in information science and technology from the Department of Information and Control, Xi'an Jiaotong University, China, in 1992, the M.S. degree in engineering in control theory and application from the Beijing University of Technology, Beijing, China, in 1998, and the Ph.D. degree from the School of Management, Tianjin University, in 2002.

In 2015, he was a Research Fellow with Drexel University, Philadelphia, PA, USA. He is currently a Full Professor, the Vice Dean of the College of Intelligence and Computing, and the Dean of the School of Computer Software, Tianjin University, China. His research interests include virtual reality, the technology of digital media content, and the Internet of Things.